Bio-based and one-day compostable poly(diethylene 2,5-furanoate) for sustainable flexible food packaging: Effect of ether-oxygen atom insertion on the final properties

Bio-based and one-day compostable poly(diethylene 2,5-furanoate) for sustainable flexible food packaging: effect of ether-oxygen atom insertion on the final properties

Silvia Quattrosoldi [a§], *Giulia Guidotti* [a§], *Michelina Soccio* [a,c*], *Valentina Siracusa* [b], *Nadia Lotti* [a,c,d]

[a]Civil, Chemical, Environmental and Materials Engineering Department, University of Bologna, Via Terracini 28, 40131 Bologna, Italy

[b]Chemical Science Department, University of Catania, Viale A. Doria 6, 95125 Catania, Italy

[c]Interdepartmental Center for Industrial Research on Advanced Applications in Mechanical Engineering and Materials Technology, CIRI-MAM, University of Bologna, Bologna, Italy

[d] Interdepartmental Center for Agro-Food Research, CIRI-AGRO, University of Bologna, Bologna, Italy.

Keywords: 2,5-furandicarboxylic acid; ether linkage; barrier properties; mechanical properties; compostability

§ These authors contributed equally.

Abstract

In the present work, the effect of ether oxygen atom introduction in a furan ring-containing polymer has been evaluated. Solvent-free polycondensation process permitted the preparation of high molecular weight poly(diethylene 2,5-furandicarboxylate) (PDEF), by reacting the dimethyl ester of 2,5-furandicarboxylic acid with diethylene glycol. After molecular and thermal characterization, PDEF mechanical response and gas barrier properties to O_2 and CO_2, measured at different temperatures and humidity, were studied and compared with those of poly(butylene 2,5-furandicarboxylate) (PBF) and poly(pentamethylene 2,5-furanoate) (PPeF) previously determined. Both PDEF and PPeF films were amorphous, differently from PBF one. Glass transition temperature of PDEF (24 °C) is between those of PBF (39 °C) and PPeF (13 °C). As concerns mechanical response, PDEF is more flexible (elastic modulus [E] = 673 MPa) than PBF (E =1290 MPa) but stiffer than PPeF (E = 9 MPa). Moreover, PDEF is the most thermally stable (temperature of maximum degradation rate being 418 for PDEF, 407 for PBF and 414 °C for PPeF) and hydrophilic (water contact angle being 74 ° for PDEF, 90 ° for PBF and 93 ° for PPeF), with gas barrier performances very similar to those of PPeF (O_2 and CO_2 transmission rate being 0.0022 and 0.0018 for PDEF and, 0.0016 and 0.0014 cm^3 cm / m^2 d atm for PPeF). Lab scale composting experiments indicated that PDEF and PPeF were compostable, the former degrading faster, in just one day.

The results obtained are explained on the basis of the high electronegativity of ether oxygen atom with respect to the carbon one, and the consequent increase of dipoles along the macromolecule.

1. Introduction

Although relatively new compared to wood, glass and metals, these last used by man since the dawn of time, plastics have been used more and more and today they are practically irreplaceable. As proof of this, their production has increased from 270 million metric tons to almost 370 million metric tons from 2010 to 2020, and it is expected to further increase, rising to about 590 million metric tons by 2050.[1,2] Their global market is also expected to reach 750.1 billion of dollars by 2028.[3] Such a massive use of plastics entails a significant impact on both exploitation of non-renewable sources and on accumulation of wastes in the marine and terrestrial habitats. The environmental problems caused by human activity are one of the main themes of debate of the last Century. With the perspective of reducing the environmental issues and building a new circular economy, the employment of renewable resources for plastic production and plastic waste recycling are the most suitable solutions. For this reason, sustainable materials are attracting a continuously growing interest as potential candidates for the replacement of traditional plastics.[4,5] To date, promising results have been obtained with bioplastics, in particular with the class of bio-based polyesters.[6,9] Their bio-based nature makes them particularly interesting for applications in food packaging field, since the multilayer structure of most of the packaging currently used creates severe recycling limits.[10] Nevertheless, to be suitable for food packaging employement, a polymeric device has to satisfy strict requirements, including proper mechanical response and outstanding barrier performance.[11] Nowadays, the so-called "smart packaging" has attracted a great interest too, as a result of lifestyle changes and consumer's desire for convenient, safe and tasty food with prolonged shelf life and unaltered quality and freshness.[12,13] In these intelligent packaging systems, added materials interact with the internal environment of the package, monitoring the state of the food inside and reducing its corruption until consuming.[14-16]

Another way to reduce environmental impact, is the use of flexible packaging instead of rigid one. A LCA study commissioned by Flexible Packaging Europe in 2021 showed that flexible packages have

a more than 60% lower impact than their rigid counterparts.[17,18] More in detail, using flexible alternatives means reducing package volumes and amount, saving space and energy during transportation and minimizing wastes. As a confirmation of this, another study, carried out by the Institute for Energy and Environmental Research in 2020, demonstrated that flexible packaging is more effective than rigid one in preserving resources and reducing carbon footprint: if all rigid packaging of non-beverage Fast Moving Consumer Goods in the European Union would be substitute by flexible one, the amount of primary packaging waste could be reduced by 21 million tonnes (i.e. 70%) per year.[18]

In this framework, furan-based polyesters can be surely considered the materials of the future,[19-24] since they can be used to produce a mono-material packaging, combining bio-based origin[25-31] with excellent barrier properties and tunable mechanical performances, ranging from high stiffness to elastomeric behavior.[32,33] More important, they can also be recycled, once the first use has been accomplished.

When employed as food containers, plastics are often contaminated with organic matter, which prevents recycling, or at least makes it very expensive,. Moreover, it must be kept in mind that an efficient and sustainable plastic waste management became more complex and difficult due to COVID-19.[34,35] The pandemic emergency , has determined a huge increase of food packaging plastic waste due to online shopping and home delivery, accompanied by a change in mindset, according to which single use plastics provides “safety”. Plastic recycling increased at slower rate for fear that plastic wastes might be infected, and due to the lockdown too.[36]

Within this scenario, which was already complex and became even more difficult due to the pandemic, compostable packaging represents the best option, especially for single-use plastics.

Aromatic polymers, such as furan-based polyesters, are hardly attacked both by water and/or microorganisms.[37-40] The development of a strategy able to enhance their modest degradation rate is a really important challenge.[41,42]

As is well known, the strong point of plastics is the unique combination of light weight, durability, low cost, ease of synthesis and the possibility to *ad hoc* modify their functional properties in view of the particular application. Even though the use of additives, physical and chemical blending and production of composites are very effective tools to properly tune the material performances,[24,43,44] the starting point is definitely represented by a proper chemical design. Minor modifications in the chemical structure of a polymer, such as the overall composition, the atomic arrangement in the backbone, the length of the subunits in the repeating unit, the presence of side-groups and isomerism can lead to significant variations in physical properties. [21,22,45-49] Macromolecular mobility and the developed microstructure are strongly connected to the chemical structure of the polymer, thus affecting features like mechanical response, thermal stability, hydrophilicity, gas barrier performance and compostability.[50]

Considering also that 2,5-furandicarboxylic acid (FDCA) is one of 12 high value-added chemicals obtained from sugars[31,51] according to the United States Department of Energy (updated in 2020),[52,53] in the present work, a new 100% renewable furan-based polyester was synthesized by two-step melt polycondensation reaction, following the "Green chemistry" principles. For this purpose, FDCA has been coupled with diethylene glycol, recently proposed as bio-based monomer,[54] obtaining poly(diethylene 2,5-furanoate) (PDEF). It is worth noting that the starting monomers, FDCA and diethylene glycol, can be derived from second and third generation cellulosic feedstocks (non-food crops, waste materials and algae), thus avoiding the exploitation of food and animal feed as well as of land destined for food production.[55] As one can see from the PDEF chemical formula (**Scheme 1A**), an ether-oxygen atom is contained in its repeating unit. As previously evidenced for other polymeric systems,[56-63] the presence of -C-O-C- moiety in the polymer backbone has several effects, such as an increase in crystallinity degree decrease and wettability. These factors can potentially favour the water/polymer affinity and, consequently, the hydrolytic and bacterial attack of the macromolecule backbone. From the chemical structure point of view, PDEF can be considered as coming from the modification of the previously studied poly(butylene 2,5-furanoate) (PBF)[33,64] and

poly(pentamethylene 2,5-furanoate) (PPeF).[32,33] In particular, PDEF can be obtained through the insertion of an O atom (centrally located) in the glycol moiety of PBF, or by substituting the central methylene group of the aliphatic subunit of PPeF with the ether-oxygen (**Scheme 1A**). To the best of our knowledge, PDEF was previously synthesized by Katia Loos' group using a lipase as catalyst, [65] and by Haernvall et al. through direct esterification, and characterized from the molecular, thermal and enzymatic degradation point of view.[66] In addition to molecular and thermal characterization, the polyester reported in the present paper was also subjected to mechanical characterization and the surface hydrophilicity of the compression molded film was also evaluated. Lab-scale composting experiments were carried out at 58°C at 90% humidity. Barrier performances to oxygen and carbon dioxide were investigated at two different temperatures (23 and 38 °C). The effect of relative humidity at 23°C was also studied. All the results obtained for PDEF were compared with the previous ones got on PBF and PPeF with the aim to evaluate the effect of this chemical modification on the final solid-state properties. The present work is meant to enlarge the furan-based polymer knowledge and, more importantly, to lay the foundations for a deep study of structure-property relationship, which is fundamental for the design of new materials addressing the desired final properties.

2. Materials and methods

2.1 Materials

Dimethyl furan-2,5-dicarboxylate (DMF) (99%), diethylene glycol (DEG) (99%), titanium tetrabutoxide (TBT), and titanium isopropoxide (TIP) were reagent-grade products. All reagents were bought from Sigma-Aldrich, except DMF, which was supplied by Matrix Fine Chemicals.

2.2 Synthesis

Poly(diethylene 2,5-furanoate) (PDEF) was synthesized through a green solvent-less two-stage polycondensation process. The reagents DMF (0.031 mol, 5.71 g) and DEG (0.062 mol, 6.58 g), in a molar ratio of 1:2, were charged in a 200 mL glass reactor, together with the catalysts TBT and TIP

(200 ppm of both). The system was continuously stirred (50 rpm) and the temperature adjusted by a silicone oil bath. A condenser cooled by liquid nitrogen was coupled to the reactor. In the first step, carried out at 180 °C and under nitrogen flow, the transesterification reactions took place and methanol was released off. After 90% of theoretical methanol was collected (i.e. 90 minutes), the pressure was progressively reduced to 0.05 mbar, while the temperature was raised up to 230 °C. In the second stage, lasting 3 hours, the reaction mass viscosity increased till a constant torque value. Afterwards, the polymer (6.5 g, 95% yield) was discharged from the reactor. A lightly coloured rubber-like solid was obtained. PBF and PPeF were previously synthesized by the authors through the same polycondensation procedure using the same catalysts.[32,33] Briefly, for PBF the glycolic molar excess was 300%, the first step was carried out at 180°C for 3 hours and the second one at 230°C for further 3 hours. In case of PPeF, a glycolic molar excess of 500% was adopted, the first step was carried out at 170°C for 3 hours while the second one at 220°C for further 2.5 hours.

The as-synthesized polymer was solubilized in chloroform and then precipitated in cold methanol, in order to remove residual catalysts and low molecular weight by-products.

2.3 Molecular characterization

Polymer chemical structure was verified by ^{1}H-nuclear magnetic resonance spectroscopy (Varian Inova 400-MHz Instrument) at room temperature using deuterated chloroform ($CDCl_3$) as solvent. The solution contains also 0.03 vol% tetramethylsilane (TMS) as an internal standard. The concentration of the polymeric solution was 0.5 wt %.

Polymer number molecular weight (M_n) and polydispersity index (Đ) were determined by a 1100 HPLC system (Agilent Technologies) equipped with PLgel 5 mm MiniMIX-C column, at 30 °C. Chloroform was used as the eluent, 0.3 mL/min flow, and sample concentrations of about 2 mg/mL were adopted. Calibration curve was obtained using polystyrene standards in the range of 800−100000 g/mol.

2.4 Thermal characterization

Differential Scanning Calorimetry (Perkin Elmer DSC6), calibrated with indium and cyclohexane standards, was used to analyse the thermal transitions by heating from -70 °C to 190 °C at 20 °C/min (I scan, resolution: 0.1 seconds between points). The sample (5 mg) was then cooled to −70 °C at 100 °C/min, and after that another heating scan was performed (II scan, resolution: 0.1 seconds between points). The glass transition temperature (T_g) and heat capacity (Δc_p) were taken as the midpoint and the height, respectively, of the heat capacity step at the glass transition. Melting temperature (T_m) and crystallization temperature (T_{cc}) were determined as the peak maximum/minimum of the endothermic/exothermic phenomena in the I and II heating scan DSC curves, respectively. The corresponding heat of fusion (ΔH_m) and heat of crystallization (ΔH_{cc}) were obtained from the total area of the DSC endothermic and exothermic signals, during the I and the II heating scans, respectively. For the determination of ΔH_m and ΔH_{cc} we have used a straight baseline.

Thermogravimetric analysis (Perkin Elmer TGA7), was employed to evaluate the thermal stability by heating 5 mg of polymer from 50 to 800°C at 10°C/min under nitrogen atmosphere (gas flow: 40 ml/min). The maximum degradation rate temperature (T_{max}) was calculated as the minimum of thermogram derivative .

2.5 Film preparation

Polymer films (2.5 g, 11 x 11 cm^2, 100 μm thickness) were obtained by compression molding the synthesized material with a laboratory press Carver C12. The polymer was heated to 100 °C, kept under 5 ton/m^2 pressure for 2 min, removed from the press and left cooled down to room temperature. Then, the films were stored at room temperature for 30 days before further characterization.

2.6 Water contact angle measurements

Water contact angle (WCA) determination was carried out on the compression moulded films using a KSV CAM101 instrument (Helsinki, Finland) at room temperature. The side profiles of deionized water drops (4 μL) on the polymer surface were analyzed just after deposition. In case of PDEF, also

192 the drop shape evolution with time was considered. At least 10 tests have been performed on different
193 film areas, from which the WCA average value ± standard deviation was determined.

194 **2.7 Mechanical characterization**

195 Tensile tests were performed on rectangular specimens (5 mm x 50 mm x 100 μm) by means of an
196 Instron 5966 testing machine with a transducer-coupled 1kN load cell (stretching rate: 10 mm/min).
197 The measurements were carried out at room temperature (23 °C) and a relative humidity of 55%.
198 Elastic modulus (E) was calculated from the initial slope of the stress-strain curve. Stress at yielding
199 (σ_y) and stress (σ_b) and elongation (ε_b) at break were also determined. These results are reported as the
200 average value ± standard deviation, obtained testing six different specimens.

201 **2.8 Barrier properties**

202 Barrier capability to oxygen and carbon dioxide was evaluated by a manometric method using a
203 Permeance Testing Device, type GDP-C (Brugger Feinmechanik GmbH), according to ASTM 1434-
204 82, DIN 53 536 and ISO/DIS 15 105-1 protocol. The measurements were performed on a film surface
205 of 78.5 cm^2, under a gas stream of 100 cm^3/min, at 23 and 38 °C, and 0 and 85 % relative humidity.
206 The results have been expressed as gas transmission rate (GTR, in cm^3 cm m^{-2} d^{-1} atm^{-1}), which defines
207 the permeability to gas of the film. The measurements were made in triplicate and the result was
208 expressed as average value ± standard deviation.

209 **2.9 Composting tests**

210 Composting studies have been carried out at 58 °C in mature compost kindly supplied by
211 HerAmbiente S.p.A. Films of about 20x20 mm^2 (50 mg) were placed in a 100 mL bottle containing
212 wet compost. Specimens were withdrawn from compost in triplicate at different time intervals,
213 washed and dried over P_2O_5.

214 **2.10 SEM investigation**

Surface characterization was carried out by scanning electron microscopy (SEM). SEM images were acquired on a desktop Phenom microscope on metal sputtered film samples glued on aluminum holders with carbon tape.

3. Results and discussion

3.1 Molecular characterization

In **Scheme 1A,** the chemical structure of poly(diethylene 2,5-furanoate) (PDEF) is reported, together with the formulas of the two homopolymers poly(butylene 2,5-furanoate) (PBF) and poly(pentamethylene 2,5-furanoate) (PPeF) to which PDEF has been compared throughout the present study. All the polyesters present a furan ring in the acid subunit, the difference being in the glycolic moiety. In case of PBF, four methylene groups are present. PDEF has the same number of -CH_2- groups, plus an ether-oxygen atom in between, this latter replaced by a methylene group in case of PPeF. PDEF could be considered as derived, on one side from PBF by the insertion of a central O atom in the glycol moiety and, on the other, from PPeF by the substitution of the central -CH_2- group with a -O- one.

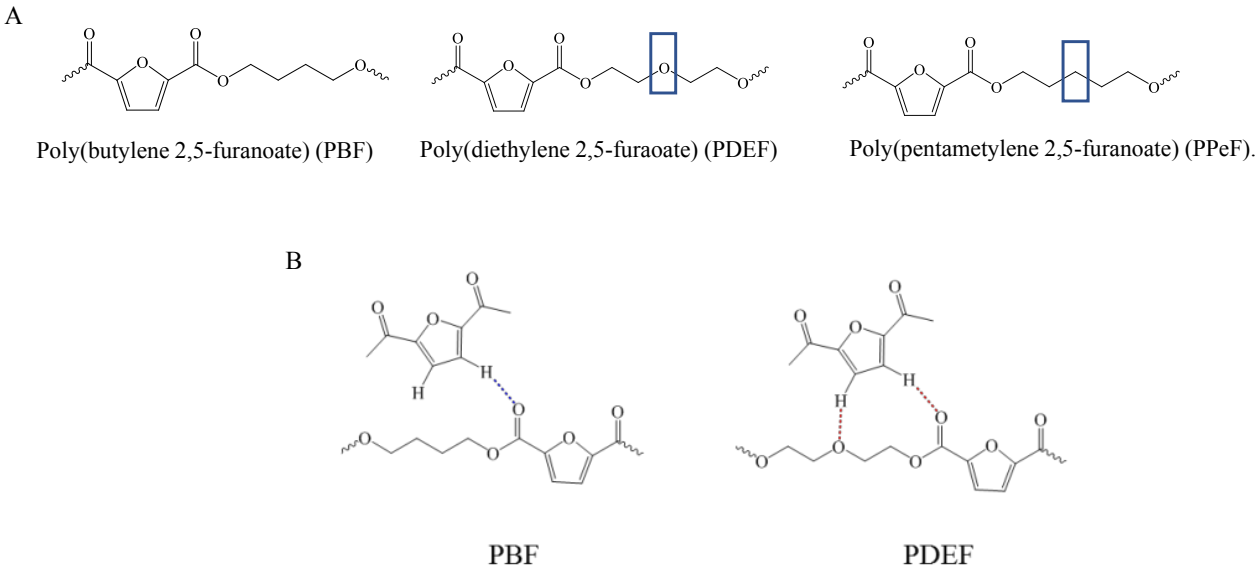

Scheme 1. A) Molecular structures of poly(diethylene 2.5-furanoate) (PDEF), poly(butylene 2,5-furanoate) (PBF) and poly(pentamethylene 2,5-furanoate) (PPeF); **B)** Inter-chain hydrogen bonds in PBF and PDEF matrices. For PPeF, a PBF-like behaviour was also supposed.

In **Fig. S1** the PDEF ^{1}H-NMR spectrum, together with the spectra of PBF and PPeF, is reported. As one can see, the expected structure for PDEF was confirmed. In details, the -CH_2- groups of the diethylene glycolic unit gave rise to two triplets at 3.82 (f) and 4.49 ppm (e), while the two d protons proper of the furan ring produced a singlet (a) located at 7.20 ppm. PBF showed the same signal at 7.34 ppm (a), then the peaks of the b and c methylene groups of the butylene subunit could be observed at 4.51 and 1.99 ppm, respectively. PPeF, beside the furan ring signal (g) at 7.20 ppm, presented three different peaks due to the methylene hydrogen atoms at 4.35 (h), 1.84 (i) and 1.57 ppm (j). The high molecular weight, obtained by means of GPC and reported in **Table 1**, confirmed the good control of the PDEF synthetic route, analogously to PBF and PPeF homopolymers.[33] The polydispersity index (Đ) resulted close to 2, as expected for a polycondensation process.

The use of traditional Titanium-based catalysts has made possible to obtain a polymer with a significantly higher molecular weight than that previously obtained by others using a lipase as catalyst.[65]

3.2 Thermal characterization

TGA analysis has been carried out to follow PDEF weight loss during heating scan under inert atmosphere (nitrogen). The corresponding thermogravimetric curve is reported in **Fig. 1A**, together with those previously obtained for PBF and PPeF, while the corresponding T_{max} values are listed in **Table 1**. The derivative curves of thermograms are reported in **Fig. S2**. It is worth noticing the high thermal stability of all the furan-based polyesters here evaluated.

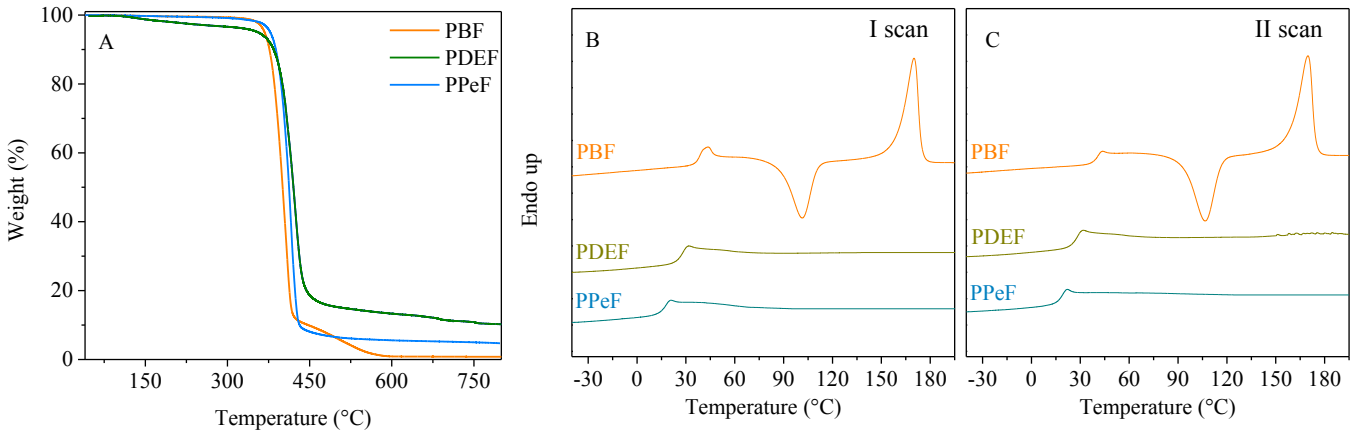

253

254 **Fig. 1. A)** Thermogravimetric analysis curves of PBF, PDEF and PPeF samples obtained by heating
255 at 10°C/min under nitrogen atmosphere; **B)** DSC traces of first heating scan of the compression
256 moulded films and **C)** second heating scan after melt quenching (20 °C/min) of PBF, PDEF, PPeF.

257

258 In agreement with previous studies,[67-69] PBF degraded at lower temperature (and comparable to the
259 one evidenced by Kainulainen et al.[64]) compared with the other two samples, reaching the maximum
260 degradation rate at 407°C, while PDEF had the highest stability despite an initial weight loss of 4%
261 occurring at approximately 100°C. The presence of -O- ether linkages along the macromolecular
262 backbone, in fact, increased the tendency of the material to absorb polar molecules as water. The
263 evaporation of the adsorbed H_2O molecules could be likely responsible for this initial weight loss
264 step in PDEF. The highest T_{max} value obtained for PDEF could be due to the higher energy of the C-
265 O bond, present in the diethylene glycol moieties, less prone to random scission compared with C-C
266 bond (358 kJ/mol vs. 346 kJ/mol, respectively[70]), proper of PBF and PPeF. Another important aspect
267 was related to the formation of inter-chain hydrogen bonds, as shown in **Scheme 1B**. The
268 establishment of inter-chain hydrogen bonds for furan-based polyesters, in addition to π-π interaction
269 between the aromatic rings, has been evidenced by dielectric experiments, rheological analysis[71] and
270 lastly proposed through simulation studies.[72] Considering the chemical structure, one can hypothesize
271 that the presence of an ether-oxygen atom in the PDEF unit could increase the hydrogen bond density,
272 thus improving the thermal resistance of the material, since the energy provided to polymer chains,

during heating, is first and preferentially used to break these physical links before breaking covalent bonds. On the contrary, the lowest thermal stability of PBF among all the samples under study could be ascribed to the lowest number of hydrogen bonds. The glassy state of PBF at room temperature could limit the establishment of such inter-chain interactions, since at 25 °C, the PBF polymer chains have lower molecular mobility than those of the rubbery PPeF sample.

Calorimetric analysis was performed in order to define the thermal transitions proper of the three samples subjected to compression molding. The DSC traces and the relative data are reported in **Fig. 1** and in **Table 1**, respectively. The cooling scans between I and II heating scans reported in **Fig. S3**. PBF film presented a melting peak centered at 164°C and preceded by a cold crystallization endotherm located at 87°C; since $\Delta H_m > \Delta H_{cc,}$ PBF film could be considered as semicrystalline. PDEF and PPeF did not present any melting peaks, showing no capability of organizing their macromolecules in crystalline structure through the compression molding process, in agreement with previous studies.[32,73] Just a glass transition step, respectively at 24 °C and 13 °C, was observed; in both cases, the values recorded were lower than the PBF one. Looking at the chemical formulas of **Scheme 1A**, one can see that PDEF and PPeF are characterized by longer glycolic subunits (PDEF: 4 -CH_2- and 1 -O-; PPeF: 5 -CH_2- moieties) compared with PBF (4 -CH_2- moieties). Even if the nature of the atom changes, longer glycols favor macromolecular mobility, moving T_g towards lower temperature.[74] $T_{g,PDEF}$ can be compared with $T_{g,PPeF}$, due to their common fully amorphous nature. As one can see, $T_{g,PDEF} > T_{g,PPeF}$, the difference due to the high electronegativity of heteroatoms in the glycolic unit of PDEF, favouring inter chain interactions (reduced chain mobility).

Despite the comparable aliphatic segment length, the highly electronegative oxygen in the glycolic portion of PDEF promoted inter-chain interactions (hydrogen bonds as well as Van der Waals interactions). In this way, the segmental relaxation was hampered, and thus glass transition temperature increased.

298

299 **Table 1.** Molecular, thermal and mechanical characterization data of PDEF, PBF and PPeF films.

300 WCA (°) and GTR values to oxygen and carbon dioxide at 23°C, RH 0% are also collected.

			PBF	PDEF	PPeF
GPC		M_n [g/mol]	27300 ±100	21400 ±100	29600 ±100
		Đ	2.3 ±0.1	2.3 ±0.1	2.4 ±0.1
TGA		T_{MAX} [°C]	407 ±1	418 ±1	414 ±1
DSC	I SCAN	T_g [°C]	39 ±1	24 ±1	13 ±1
		ΔC_p [J/g·°C]	0.24±0.01	0.45±0.01	0.39±0.01
		T_{cc} [°C]	102 ±1	/	/
		ΔH_{cc} [J/g]	26 ±1	/	/
		T_m [°C]	170 ±1	/	/
		ΔH_m [J/g]	35 ±1	/	/
	II SCAN	T_g [°C]	39 ±1	24 ±1	13 ±1
		ΔC_p [J/g·°C]	0.28±0.01	0.47±0.01	0.43±0.01
		T_{cc} [°C]	107 ±1	/	/
		ΔH_{cc} [J/g]	30 ±1	/	/
		T_m [°C]	170 ±1	/	/
		ΔH_m [J/g]	35 ±1	/	/
Tensile test		σ_y [MPa]	11 ± 2	7 ± 1	/
		σ_b [MPa]	21 ± 3	4 ± 0.2	6 ± 1
		ε_b [%]	157 ± 10	502 ± 100	1050 ± 200
		E [MPa]	1290 ± 140	673 ± 76	9 ± 1
WCA		Θ [°]	90 ± 2	74 ± 1	93 ± 3
Barrier properties		O_2-TR [cm^3 cm / m^2 d atm]	0.10 ± 0.006	0.0022 ± 0.0002	0.0016 ± 0.0001
		CO_2-TR [cm^3 cm / m^2 d atm]	0.19 ± 0.01	0.0018 ± 0.0001	0.0014 ± 0.0001

301

302

The three molten samples were subjected to fast cooling and analysed during a second heating measurement. As expected, PDEF and PPeF resulted again completely amorphous. As concerns PBF, a major polymer fraction could be quenched in the amorphous phase thanks to the high cooling rate, even though no completely amorphous sample could be obtained. As evidenced by II scan DSC trace, once T_g was exceeded, PBF macromolecules were able to fold in an ordered structure (T_{cc} = 107 °C; ΔH_{cc} = 30 J/g) which melts at higher temperature (T_m= 170°C; ΔH_m = 35 J/g). Despite the high cooling rate, ΔH_m still keeps slightly higher than ΔH_{cc}.

3.3 Mechanical characterization

Stress-strain measurements were conducted on PDEF films. The obtained curve is reported in **Fig. 2**, while the related data are collected in **Table 1**, together with the results previously got for PBF and PPeF samples. In details, PBF film showed high elastic modulus and stress at break, and quite low deformation at break in line with its semicrystalline nature, together with a T_g above room temperature. Differently, thanks to its amorphous nature and a T_g below room temperature, PPeF was characterized by an elastic modulus reduced by two orders of magnitude, together with an outstanding elongation at break (more than 1000 %). Moreover, as previously reported,[32] PPeF was able to recover its initial shape thanks to a supramolecular 1-D, 2-D structure springing from inter-chain hydrogen bonds established between macromolecular chains. PDEF had a mechanical behavior intermediate between the one typical of a semicrystalline material, as PBF, and that of a rubbery fully amorphous polymer, as PPeF. Like PBF, PDEF undergoes yielding,[75,76] a phenomenon which was not observed in PPeF. The lack of crystallites in PDEF produced a reduction of E and σ_y compared to PBF. This decrement was contained by the interactions among different chains, thanks to the oxygen atom of the glycolic subunit, which helped keeping the elastic modulus and the strain before yielding quite high. At the same time, the higher chain mobility of PDEF with respect to PBF (lower T_g), coming from the introduction of O atom, allowed reaching a 500% ε_b.

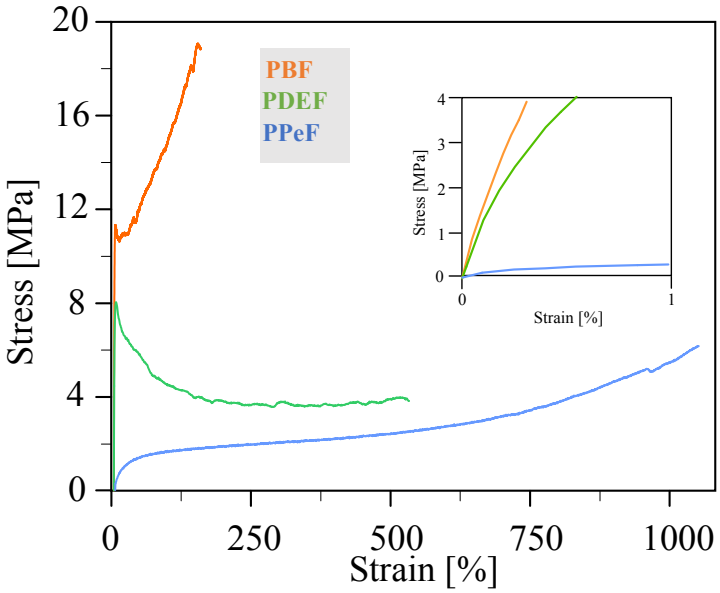

Fig. 2. Stress-strain curves of PBF, PDEF and PPeF films. In the inset the region corresponding to low values of stress and strain is reported.

3.4 Water contact angle

In order to evaluate the surface hydrophilicity of PDEF film, the interaction between film and water was investigated through water contact angle measurements. Particular attention was devoted to the effect of the introduction of an oxygen atom in the polymer backbone. Again, the outcomes obtained for PDEF film have been compared with the PBF and PPeF ones.

As it is clearly visible from **Fig. 3A** and from the data in **Table 1**, PDEF resulted the most hydrophilic film, being the WCA_{PDEF} lower than both WCA_{PBF} and WCA_{PPeF}. These results suggest that the introduction of ether-oxygen in the PBF repeating unit increases the polarity of the material, as already suggested by previous studies.[77]

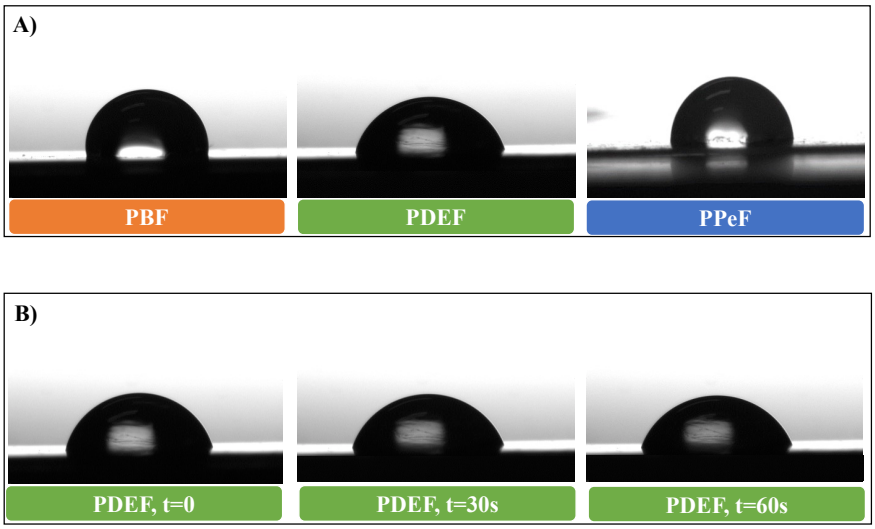

Fig. 3. A) Images of water drops deposited on PBF, PDEF and PPeF films; **B)** water drop on PDEF after 0, 30 and 60 s from deposition.

The high affinity with water was in line with the TGA results obtained for PDEF. The initial weight loss observed during the thermogravimetric analysis can be ascribed to the release of the humidity absorbed from the environment. By replacing the oxygen atom of the PDEF glycolic subunit with a non-polar -CH_2- group, obtaining the PPeF chemical structure, the hydrophobic character rose again. WCA value of PPeF is similar to that of PBF, despite the greater length of the aliphatic portion (4 -CH_2- for PBF *vs.* 5 -CH_2- for PPeF).

In **Fig. 3B**, the profile change of the drop deposited on PDEF film as a function of time was reported. A clear difference in contact angle could be observed just after 30 s from the release of the water drop. A completely different behaviour was observed for PPeF and PBF, for both of which no evolution of the drop shape with time was detected. The drop shape evolution on PDEF surface is further evidence of its improved hydrophilicity with respect to PBF and PPeF.

3.5 Composting test

In order to evaluate the potential end-of-life destination of PDEF-based products, composting tests were conducted. For each sample, square shaped films were incubated in adequately prepared compost and maintained under controlled atmosphere (58°C, 90% relative humidity). Then, several

withdrawals were operated at different times (**Fig. 4**). The composting measurements were also carried out on PBF and PPeF samples. As regards PBF, after 62 days in compost, no changes on the film surface nor in the gravimetric weight were observed.

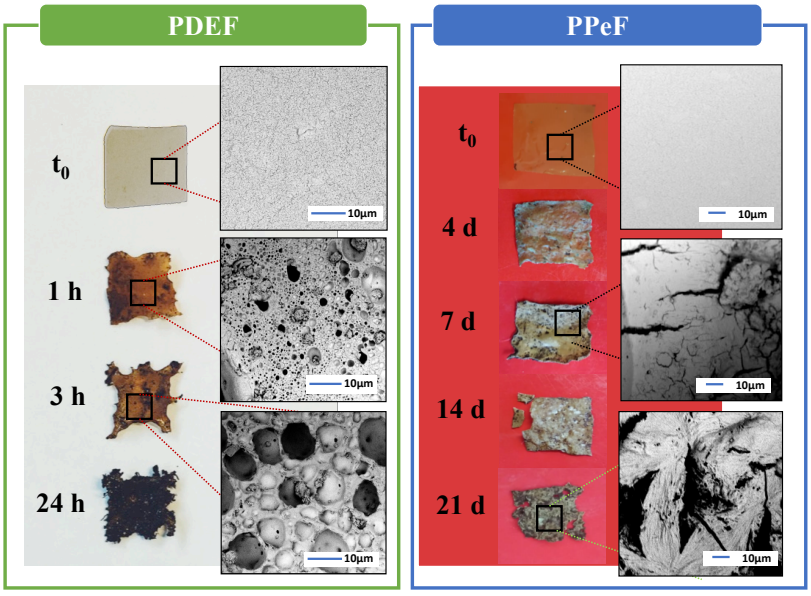

Fig. 4. PDEF and PPeF film images collected at different composting times: macroscopic view (left) and SEM images (right).

A deeply different behaviour was observed for PDEF, which underwent degradation as soon as incubated (**Fig. 4**). Just after 1 hour, the film macroscopically changed in colour and dimension, holes and cracks were clearly observed with SEM. In particular, the cavities increased in size with the incubation time, and after just 3 hours, the surface was almost completely covered of holes. After 24 hours of incubation, the film was wholly incorporated in compost. The high tendency to degrade comes from the high hydrophilicity of PDEF given by the oxygen atoms inserted in the glycolic subunit, and from the rubbery state of the polymer under the experimental conditions. Both these features favour the diffusion of water molecules and microorganisms' attack. It is worth noting that PDEF film did not undergo solubilization, as confirmed by additional experiments carried out in neat water. In this case, no changes in PDEF film both at micro- and macroscopic level were observed,

even after months. As concerns PPeF, its degradation proceeded very fast, but at lower extent compared with PDEF. Also in this case $T_{incubation} > T_{g,PPeF}$, but degradation was slowed down likely because of the lower hydrophilicity. Anyway, after 4 days, macroscopical changing on the film surface could be seen and, after 7 days, cracks and holes could be observed microscopically via SEM analysis. In 21 days, the film was deeply compromised by degradation process both at micro- and macroscopic level (**Fig. 4**). Given the compost contamination of the incubated PDEF and PPeF films, it was not possible to perform weight loss measurements.

The huge slowing down of composting rate for PBF films has to be ascribed to its semicrystalline nature and lower macromolecular mobility ($T_{g,PBF} > T_{g,PDEF,} T_{g,PPeF}$) more than to its quite high hydrophobicity, being this last comparable to PPeF one ($WCA_{PBF} \approx WCA_{PPeF}$).

3.6 Barrier properties

Barrier properties are influenced by several factors that can have different impact on the final performance. As a general trend, all factors that increase free volume among chains worsen barrier properties. A pertinent example is the macromolecule flexibility, which is related to the glass transition temperature. In particular, the lower the T_g the higher the number of unoccupied spaces, which cause the increase of gas transmission rate (GTR). Differently, the presence of ordered phases hampers the passage of gases through the film. In addition to the three-dimensional crystals, in the systems containing aromatic or aliphatic rings connected by flexile moieties, 1D- and 2D-ordered phases can develop, arising from Van der Waals forces, π-π stacking and polar interactions.[78-82] Barrier properties also depend on the possibility of ring flipping,[83] and of macromolecular arrangements, which may affect the overall dipolar moment without changing the chemistry.[84] In addition to them, in the case of furan-based polymers, the establishment of hydrogen bonds can be also considered.[32,33,71,72] PDEF gas barrier properties were analysed and compared with those of PBF and PPeF.

The permeability performances to two different pure gases, O_2 and CO_2, were evaluated on the compression moulded films. In **Fig. 5A** the results, expressed as gas transmission rate (GTR), were

402 reported. The experiments were conducted sequentially, as follows: i) temperature (T) 23°C, relative
403 humidity (RH) 0%; ii) T 23°C, RH 85%; iii) T 23°C, RH 0%. From the first test conducted at 23°C
404 in dry atmosphere, it was clear that PBF presented the highest values of GTR among the series, despite
405 its higher glass transition temperature and semicrystalline nature. Differently, PDEF and PPeF, even
406 though amorphous and with T_g values around the temperature of measuring, resulted very outstanding
407 and with comparable performance. An explanation could be found, as mentioned before, in the
408 presence of a particular macromolecular arrangement that blocked the passage of gases through the
409 materials.[85] In the case of PPeF, as previously reported,[32,33] 1-D, 2D-ordered domains developed
410 during compression moulding with consequent improvement of gas barrier performance. This
411 peculiar microstructure originated from inter-chain hydrogen bonds, these last also present, and to
412 greater extent, in PDEF. The presence of ether-oxygen atom in PDEF repeating unit enhanced the
413 number of hydrogen bonds favouring the inter-molecular forces. These last lead to a compact array,
414 that hampered the gas molecules passage. At the same time, the insertion of an oxygen atom into the
415 glycol subunit decreases the symmetry of the aliphatic segment, reducing the macromolecular sorting.
416 In other words, the density of the inter-chain hydrogen bond increases due to the presence of ether O
417 atoms, but their random distribution determines a not enough long chain arrangement, not detectable
418 through diffractometric measurements. Nevertheless, unexpectedly, the barrier performances of the
419 PDEF were not superior to those of PPeF. The result could be explained considering that the
420 formation of the compact array is somewhat contrasted by the lower mobility of the PDEF
421 macromolecular chains compared to those of the PPEF ($T_{g,PDEF} > T_{g,PPeF}$).
422 Afterwards, the three films were subjected to permeability tests at 85% RH, keeping the temperature
423 constant at 23°C. In case of PBF, an improvement of barrier performance was observed, while for
424 PDEF, permeability values remained almost constant. The result was quite surprising considering the
425 usually observed plasticizing effect of water, which, enhancing the chain mobility, determined an
426 increment of the free volume. On the other side, the same plasticizing effect detected for PPeF, caused
427 a slight increase of GTR values under humid conditions. To explain the behaviour of PDEF and PBF

428 films, it was supposed that water enhanced the inter-chain interactions occupying the empty sites at
429 the oxygen atoms of the furan ring and, in case of PDEF, also at the oxygen of the glycolic subunit.
430 Hence, a more compact and dense new structure was formed, responsible for the decreasing of the
431 GTR values.[85] In the case of PPeF, also containing furan O atoms in the furan ring, the longer glycolic
432 part compared to PBF decreased the density of furan ring per unit length. Therefore, the plasticizing
433 effect of water prevailed on the formation of a more compact microstructure arising from the
434 hydrogen bonds establishment. In PDEF, characterized by repeating unit length comparable to PPeF,
435 the presence of the oxygen atom instead of the central methylene group explained the different
436 behaviour in wet environment.
437 In the third experiment, the films were firstly subjected to vacuum in order to remove the moisture
438 residues and then, a new test was performed at 23°C and 0% RH. PBF and PDEF maintained the
439 same good performances reached under humid conditions. It is plausible that the vacuum applied was
440 not affecting the hydrogen bonds formed among water and furan/ether oxygen. For PPeF, it could be
441 hypothesized that the free molecules of water trapped inside the material and acting as plasticizer,
442 were removed by vacuum. Conversely, those forming hydrogen bonds with the furan ring remained
443 inside the material, making GTR-O_2 value decrease and GTR-CO_2 one almost unvaried.
444 Another aspect to consider was the different perm-selectivity ratio, defined as GTR_{CO_2}/GTR_{O_2}, which
445 is an indication of the different barrier performance towards the two gases. It should be remembered
446 that oxygen is a small and no-polar molecule characterized by a transmission rate lower than that of
447 the larger carbon dioxide, which contains polar C-O covalent bonds.[50] Consequently, the perm-
448 selectivity ratio is usually higher than 1. Usually, in polyesters $GTR_{CO_2} > GTR_{O_2}$, meaning carbon
449 dioxide passed through the films easier than O_2. In the furan-based polyesters, a peculiar behaviour
450 with particularly low GTR values for CO_2 had been documented.[32,86-88] This evidence was ascribed
451 to the presence of permanent dipoles in CO_2 interacting with the polar groups of polymeric chains

(furan ring), thus increasing CO_2 solubility and simultaneously decreasing its diffusivity. The consequent result is a GTR_{CO_2}/GTR_{O_2} ratio close to 1 for furan-containing polyesters.

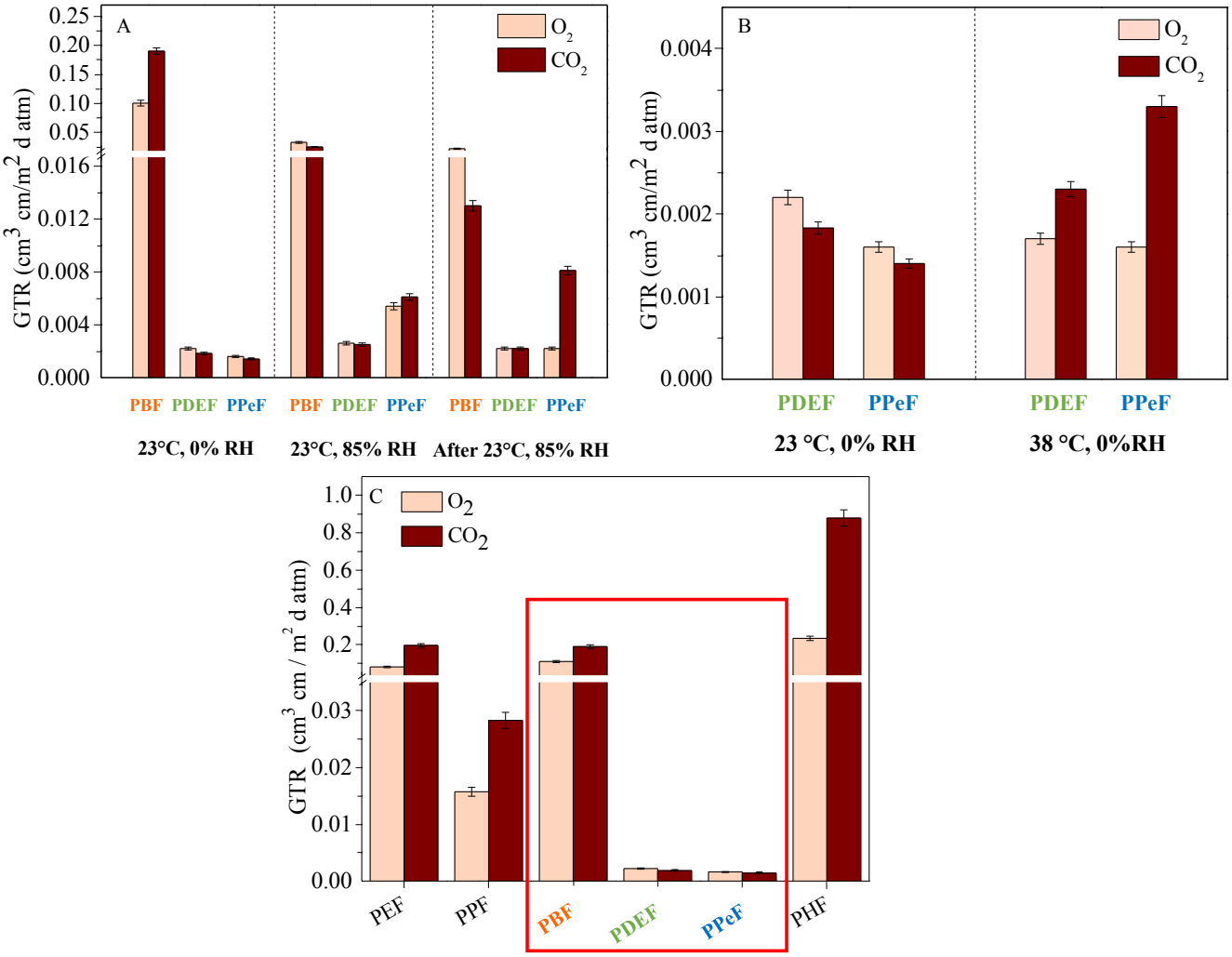

Fig. 5. A) GTR-O_2 and -CO_2 of PBF, PDEF and PPeF, for three subsequent experiments conducted at 23°C in different conditions of humidity; **B)** GTR-O_2 and -CO_2 of PDEF and PPeF at 23 and 38 °C; **C)** GTR-O_2 and -CO_2 of different furan-based polyesters (PEF[34], PPF[10], PHF[10]).

Considering the three-step experiment reported in **Fig. 5A**, a different effect of humidity conditions on perm-selectivity ratio could be found for PBF, PDEF and PPeF films.

As concerns PBF, in the first test conducted, the driving force was the dimension of the molecules. Operating at 85% RH, new polar interactions between water molecules and polymer chains formed, favouring CO_2 solubility. The effect kept constant even returning to dry environment.

In case of PDEF, its higher polarity due to the O atom insertion in the PBF backbone, helped to maintain the $GTRc_{O_2}/GTR_{O_2}$ ratio always close to 1. As regards PPeF, the trend observed was different: humidity determined an increment of perm-selectivity ratio, which further increased after removing free water molecules by vacuum. This trend could be explained considering that H_2O first acted as plasticizer, enhancing polymer chain mobility, and then left vacancies after vacuum was applied. Both these effects increased the free volume, favouring mainly the passage of the fastest CO_2 molecules. These last, in turn, were less soluble in PPeF than in PBF and especially in PDEF films.

PDEF and PPeF were also tested at 38°C to simulate hot weather conditions. As one can see from **Fig. 5B**, despite at this temperature macromolecular chains of both polymers were in a complete mobile state, barrier properties did not suffer a general worsening. This experiment supports, one more time, the hypothesis of supramolecular arrays originated from hydrogen bonds among the chains. As evident, these compact structures were not affected by the increasing of temperature, since the polymers maintain their performances. Differently, the increase of temperature in case of common polyesters leads to higher free volume among the macromolecules, favouring gas permeation.

Anyway, an increase of CO_2 gas transmission rate was detected by increasing temperature. As already mentioned, the gas passage depended on both solubility and diffusivity. This latter generally rises with temperature, the effect being more intense for the gas molecules characterized by the most chaotic motions, such as CO_2 molecules. In both cases, the performances to O_2 at 23°C and 38°C were constant, while GTR_{CO_2} values increased.

In **Fig. 5C**, a comparison of PDEF with PBF, PPeF and other furan-based polyesters was reported. As one can see, PDEF and PPeF had GTR values much lower than the other materials.

In addition, an odd/even effect could be observed: the materials with odd number of -CH_2- groups resulted more performant compared to the even numbered -CH_2- containing ones. Surprisingly, PDEF and PPeF presented GTR values lower than those of PPF, despite their lower T_g ($T_{g,PPeF}$ = 13°C; $T_{g,PDEF}$ = 24°C; $T_{g,PPF}$ = 52°C). As previously reported, the deviating behaviour of PPeF and PDEF could be attributed to the supramolecular compact phase coming from the hydrogen bond formation, this last being favoured in rubbery amorphous furan-polyesters as PDEF and PPeF.

As regards the materials containing an even number of -CH_2- groups, PEF, PBF and PHF, a progressive worsening of gas barrier performances can be observed, ascribable to different reasons as previously reported:[33,89] (i) increasing amount of the so called disclinations; (ii) increasing fraction of 3D-ordered phase at the expense of the more performant 2D-one; (iii) increasing of free volume fraction ($T_{g,PEF}$>$T_{g,PBF}$ >$T_{g,PHF}$).

4. Conclusions

The use of traditional synthetic Ti-based catalysts together with an optimized solvent-free two-stage polycondensation process permitted to obtain a 100% bio-based high molecular weight poly(diethylene 2,5-furanoate) (PDEF). The polymer could be processed in form of thin freestanding films by compression moulding, although completely amorphous and with a T_g around room temperature. A similar behaviour was previously observed for poly(pentamethylene 2,5-furanoate) (PPeF), with respect to which the polymer object of this study has some important similarities in terms of properties. In particular, both polyesters are characterized by very high thermal stability (PDEF's one even slightly higher than that of PPeF), exceptional gas barrier properties both at room temperature and at 38°C, preserved in the presence of humidity. Lastly, they are both compostable, although PDEF degrades much faster than PPeF, mainly due to its greater hydrophilicity. In terms of mechanical response, a fundamental property for a possible application in food packaging, PDEF showed an intermediate behaviour between poly(butylene 2,5-furanoate) (PBF) and PPeF. In fact, PDEF film exhibited the flexibility typical of PPeF, even though not an elastomeric behaviour (PDEF

stress-strain curve shows yielding), but a much higher elastic modulus and stress at break as PBF, which confer to the material toughness and ductility. Therefore, with PDEF both the mechanical limits of PBF (brittleness) and of PPeF (too high softness) are overcome, without compromising the outstanding thermal stability, gas barrier properties and compostability of PPeF. The goal was achieved through a small chemical modification of polymer chemical structure, i.e. the insertion of an ether oxygen atom into the glycol subunit, centrally positioned. As known from basic chemistry, oxygen is characterized by high electronegativity and small dimensions, and these characteristics have had a significant impact on the final properties of the polymer. Specifically:

- The lower dimension of oxygen with respect to carbon atom affected the chain constitutional regularity with consequent suppression of the polymer crystallization capacity (PDEF is amorphous, whereas PBF is semicrystalline). Moreover, C-O bond is shorter than C-C one, implying for ethereal bond a higher energy (PDEF is more thermally stable than PBF); the insertion of an oxygen atom in glycol subunit also makes its polymer chain more flexible than that of PBF, the aliphatic part being longer;
- The high oxygen electronegativity strengthens inter-chain interactions (hydrogen bonds involving furan ring and Van der Waals interactions) responsible of the outstanding gas barrier (similar to those of PPeF) and mechanical properties (better than those of both PBF and PPeF) and increases polymer hydrophilicity, the parameter determining the very fast compostability of this polyester.

In conclusion, PDEF represents a very promising candidate to obtain an easily recyclable mono-material package and also for producing single-use plastic packaging compostable in just one day.

Author contributions

S.Q. M.S. synthesized and characterized the polymer. V.S. performed gas barrier measurements. S.Q., G.G., M.S. and N.L. analyzed the overall experimental data. M.S. and N.L. wrote manuscript. G.G., M.S. and N. L. corrected and reviewed the manuscript. N.L. supervised and financed the work.

Conflicts of interest

The authors declare no conflict of interests.

Acknowledgments

S.Q, G.G., M.S., N.L., and V.S. acknowledge the Italian Ministry of University and Research. This publication is based upon work from COST Action FUR4Sustain, CA18220, supported by COST (European Cooperation in Science and Technology).

The authors thank Dr. Massimo Gazzano for his cooperation in the acquisition of SEM micrographs.

Supplementary data

These files can be found in the supplementary data:

Fig. S1. ^{1}H-NMR spectra of PBF, PDEF and PPeF (from the top to the bottom) with the relative peak assignment.

References

1. Plastics - The facts 2020. *PlasticsEurope,* 2020, https://www.plasticseurope.org/en/resources/publications/4312-plastics-facts-2020 (accessed July 2021).
2. https://www.statista.com/statistics/664906/plastics-production-volume-forecast-worldwide/ STATISTA 2021 (accessed September 2021).
3. Plastic Market Size, Share & Trends Analysis Report by Product (PE, PP, PU, PVC, PET, Polystyrene, ABS, PBT, PPO, Epoxy Polymers, LCP, PC, Polyamide), by Application, by

End-use, by Region, and Segment Forecasts, 2021 – 2028, Grand view Research 2021 (accessed: September 2021).

4. RameshKumar, S.; Shaiju, P.; O'Connor, K. E.; P, R. B. Bio-Based and Biodegradable Polymers - State-of-the-Art, Challenges and Emerging Trends. *Curr. Opin. Green Sustain. Chem*. **2020**, *21*, 75–81.
5. Mülhaupt, R. Green Polymer Chemistry and Bio-based Plastics: Dreams and Reality. *Macromol. Chem. Phys*. **2013**, *214*, 159–174.
6. Rabnawaz, M.; Wyman, I.; Auras, R.; Cheng, S. A roadmap towards green packaging: the current status and future outlook for polyesters in the packaging industry. *Green Chem*. **2017**, *19*, 4737-4753.
7. Álvarez-Chávez, C. R.; Edwards, S.; Moure-Eraso, R; Geiser, K. Sustainability of bio-based plastics: General comparative analysis and recommendations for improvement. *J. Clean Prod*. **2012**, *23*, 47–56.
8. Papageorgiou, G. Z. Thinking Green: Sustainable Polymers from Renewable Resources. *Polymers* **2018**, *10*, 952.
9. Zhang, Q.; Song, M.; Xu, Y.; Wang, W.; Wang, Z.; Zhang, L. Bio-based polyesters: Recent progress and future prospects. *Prog. Polym. Sci*. **2021**, *120*, 101430.
10. Morris, A. B. *The Science and Technology of Flexible Packaging. Multilayer Films from Resin and Process to End Use,* Elsevier, **2016**.
11. Reichert, C. L.; Bugnicourt, E.; Coltelli, M.-B.; Cinelli, P.; Lazzeri, A.; Canesi, I.; Braca, F.; Martínez, B. M.; Alonso, R.; Agostinis, L.; Verstichel, S.; Six, L.; De Mets, S.; Gómez, E. C.; Ißbrücker, C.; Geerinck, R.; Nettleton, D. F.; Campos, I.; Sauter, E.; Pieczyk, P.; Schmid, M. Bio-Based Packaging: Materials, Modifications, Industrial Applications and Sustainability. *Polymers* **2020**, *12*, 1558.
12. Young, E.; Mirosa, M.; Bremer, P. A Systematic Review of Consumer Perceptions of Smart Packaging Technologies for Food. *Front. Sustain. Food Syst*. **2020**, *4*, 63.

584 13. Majid, I.; Nayik, G. A.; Dar, S. M.; Nanda, V. Novel food packaging technologies:
585 Innovations and future prospective. *J. Saudi Soc. Agric. Sci*. **2018**, *17*, 454-462.
586 14. Bhargava, N.; Sharanagat, V. S.; S Mor, R.; Kumar, K. Active and intelligent biodegradable
587 packaging films using food and food waste-derived bioactive compounds: A review. *Trends*
588 *Food Sci. Technol*. **2020**, *105*, 385-401.
589 15. Firouz, M. S.; Mohi-Alden, K.; Omid, M. A critical review on intelligent and active packaging
590 in the food industry: Research and development. *Food Res. Int*. **2021**, *141*, 110113.
591 16. Singh, G.; Singh, S.; Kumar, B.; Gaikwad, K. K. Active barrier chitosan films containing
592 gallic acid based oxygen scavenger. *J. Food Meas. Charact*. **2021**, *15*, 585–593.
593 17. https://perfectpackaging.org (accessed: September 2021).
594 18. https://www.flexpack-europe.org (accessed: September 2021).
595 19. Vilela, C.; Sousa, A. F.; Fonseca, A. C.; Serra, A. C.; Coelho, J. F. J.; Freire, C. S. R.;
596 Silvestre, A. J. D. The quest for sustainable polyesters – insights into the future. *Polym. Chem*.
597 **2014**, *5*, 3119-3141.
598 20. Hwang, K. R.; Jeon, W.; Lee, S. Y.; Kim, M. S.; Park, Y. K. Sustainable bioplastics: Recent
599 progress in the production of bio-building blocks for the bio-based next-generation polymer
600 PEF. *Chem. Eng. J.* **2020**, *390*, 124636.
601 21. Sousa, A. F.; Vilela, C.; Fonseca, A. C.; Matos, M.; Freire, C. S. R.; Gruter, G. J. M.; Coelho,
602 J. F. J.; Silvestre, A. J. D. Biobased polyesters and other polymers from 2,5-furandicarboxylic
603 acid: a tribute to furan excellency. *Polym. Chem*. **2015**, *6*, 5961-5983.
604 22. Papageorgiou, G. Z.; Papageorgiou, D. G.; Terzopoulou, Z.; Bikiaris, D. N. Production of bio-
605 based 2,5-furan dicarboxylate polyesters: Recent progress and critical aspects in their
606 synthesis and thermal properties. *Eur. Polym. J*. **2016**, *83*, 202-229.
607 23. Loos, K.; Zhang, R.; Pereira, I.; Agostinho, B.; Hu, H.; Maniar, D.; Sbirrazzuoli, N.; Silvestre,
608 A. J. D.; Guigo, N.; Sousa, A. F. A Perspective on PEF Synthesis, Properties, and End-Life.
609 *Front. Chem*. **2020**, *8*, 585.

24. Terzopoulou, Z.; Papadopoulos, L.; Zamboulis, A.; Papageorgiou, D. G.; Papageorgiou, G. Z.; Bikiaris, D. N. Tuning the Properties of Furandicarboxylic Acid-Based Polyesters with Copolymerization: A Review. *Polymers* **2020**, *12*, 1209.
25. Iglesias, J.; Martínez-Salazar, I.; Maireles-Torres, P.; Martin Alonso, D.; Mariscal, R; López Granados, M. Advances in catalytic routes for the production of carboxylic acids from biomass: a step forward for sustainable polymers. *Chem. Soc. Rev*. **2020**, *49*, 5704-5771.
26. Chen, C.; Wang, L.; Zhu, B.; Zhou, Z.; El-Hout, S. I.; Yang, J.; Zhang, J. 2,5-Furandicarboxylic acid production via catalytic oxidation of 5-hydroxymethylfurfural: Catalysts, processes and reaction mechanism. *J. Energy Chem*. **2021**, *54*, 528-554.
27. Wojcieszak, R.; Itabaiana, I. Engineering the future: Perspectives in the 2,5-furandicarboxylic acid synthesis. *Catal. Today* **2020**, *354*, 211-217.
28. Dedes, G.; Karnaouri, A.; Topakas, E. Novel Routes in Transformation of Lignocellulosic Biomass to Furan Platform Chemicals: From Pretreatment to Enzyme Catalysis. *Catalysts* **2020**, *10*, 743.
29. Wu, S.; Liu, Q.; Tan, H.; Zhang, F.; Yin, H. A Novel 2,5-Furandicarboxylic Acid Biosynthesis Route from Biomass-Derived 5-Hydroxymethylfurfural Based on the Consecutive Enzyme Reactions. *Appl. Biochem. Biotechnol*. **2020**, *191*, 1470–1482.
30. Naim, W.; Schade, O. R.; Saraci, E.; Wust, D.; Kruse, A.; Grundwaldt, J. D. Toward an Intensified Process of Biomass-Derived Monomers: The Influence of 5-(Hydroxymethyl)furfural Byproducts on the Gold-Catalyzed Synthesis of 2,5-Furandicarboxylic Acid. *ACS Sustainable Chem. Eng*. **2020**, *8*, 11512–11521.
31. Deshan, A. D. K.; Atanda, L.; Moghaddam, L.; Rackemann, D. W.; Beltramini, J.; Doherty, W. O. S. Heterogeneous Catalytic Conversion of Sugars Into 2,5-Furandicarboxylic Acid. *Front. Chem*. **2020**, *8*, 659.
32. Guidotti, G.; Soccio, M.; García-Gutiérrez, M. C.; Gutiérrez-Fernández, E.; Ezquerra, T. A.; Siracusa, V.; Munari, A.; Lotti, N. Evidence of a 2D-Ordered Structure in Biobased

636 Poly(pentamethylene furanoate) Responsible for Its Outstanding Barrier and Mechanical
637 Properties. *ACS Sustainable Chem. Eng*. **2019**, *7*, 17863−17871.
638 33. Guidotti, G.; Soccio, M.; García-Gutiérrez, M. C.; Ezquerra, T.; Siracusa, V.; Gutiérrez-
639 Fernández, E.; Munari, A.; Lotti, N. Fully Biobased Superpolymers of 2,5-Furandicarboxylic
640 Acid with Different Functional Properties: From Rigid to Flexible, High Performant
641 Packaging Materials. *ACS Sustainable Chem. Eng.* **2020**, *8*, 9558–9568.
642 34. Benson, N. U.; Bassey D. E.; Palanisami, T. COVID pollution: impact of COVID-19
643 pandemic on global plastic waste footprint. *Heliyon* **2021**, *7*, e06343.
644 35. Klemeš, J. J.; Van Fan, Y.; Tan, R. R.; Jiang, P. Minimising the present and future plastic
645 waste, energy and environmental footprints related to COVID-19. *Renewable Sustainable*
646 *Energy Rev*. **2020**, *127*, 109883.
647 36. Khoo, K. S.; Ho, L. Y.; Lim, H. R.; Leong, H. Y.; Chew, K. W. Plastic waste associated with
648 the COVID-19 pandemic: Crisis or opportunity? *J. Hazard. Mater*. **2021**, *417*, 126108.
649 37. Pellis, A.; Haernvall, K.; Pichler, C. M.; Ghazaryan, G.; Breinbauer, R.; Guebitz, G. M.
650 Enzymatic hydrolysis of poly(ethylene furanoate). *J. Biotechnol.* **2016**, *235*, 47-53.
651 38. Gigli, M.; Quartinello, F.; Soccio, M.; Pellis, A.; Lotti, N.; Guebitz, G. M.; Licoccia, S.;
652 Munari, A. Enzymatic hydrolysis of poly(1,4-butylene 2,5-thiophenedicarboxylate) (PBTF)
653 and poly(1,4-butylene 2,5-furandicarboxylate) (PBF) films: A comparison of mechanisms.
654 *Environ. Int*. **2019**, *130*, 104852.
655 39. Okada, M.; Tachikawa, K.; Aoi, K. Biodegradable polymers based on renewable resources.
656 II. Synthesis and biodegradability of polyesters containing furan rings. *J. Polym. Sci., Part A:*
657 *Polym. Chem*. **1997**, *35*, 2729−2737.
658 40. Muller, R. J.; Kleeberg, I.; Deckwer, W. D. Biodegradation of polyesters containing aromatic
659 constituents. *J. Biotechnol*. **2001**, *86*, 87–95.

660 41. Soccio, M.; Costa, M.; Lotti, N.; Gazzano, M.; Siracusa, V.; Salatelli, E.; Manaresi, P.;
661 Munari, A. Novel fully biobased poly(butylene 2,5-furanoate/diglycolate) copolymers
662 containing ether linkages: Structure-property relationships. *Eur. Polym. J.* **2016**, *81*, 397–412.
663 42. Guidotti, G.; Soccio, M.; Lotti, N.; Siracusa, V.; Gazzano, M.; Munari, A. New multi-block
664 copolyester of 2,5-furandicarboxylic acid containing PEG-like sequences to form flexible and
665 degradable films for sustainable packaging. *Polym. Degrad. Stab.* **2019**, *169*, 108963.
666 43. Cowie, J. M. G.; Arrighi, V. *Polymers Chemistry and Physics of Modern Materials*, 3rd
667 Edition, CRC Press, **2007**, Chapter 15.
668 44. Poulopoulou, N.; Smyrnioti, D.; Nikolaidis, G. N.; Tsitsimaka, I.; Christodoulou, E.; Bikiaris,
669 D. N.; Charitopoulou, M. A.; Achilias, D. S.; Kapnisti, M.; Papageorgiou, G. Z. Sustainable
670 Plastics from Biomass: Blends of Polyesters Based on 2,5-Furandicarboxylic Acid. *Polymers*
671 **2020**, *12*, 225.
672 45. Thiyagarajan, S.; Vogelzang, W.; Knoop, R. J. I.; Frissen, A. E.; van Haveren, J.; van Es, D.
673 S. Biobased furandicarboxylic acids (FDCAs): effects of isomeric substitution on polyester
674 synthesis and properties. *Green Chem*. **2014**, *16*, 1957-1966.
675 46. Soccio, M.; Nogales, A.; García-Gutiérrez, M.; Lotti, N.; Munari, A.; Ezquerra, T. Origin of
676 the subglass dynamics in aromatic polyesters by labeling the dielectric relaxation with ethero
677 atoms. *Macromolecules* **2008**, *41*, 2651–2655.
678 47. Bianchi, E.; Soccio, M.; Siracusa, V.; Gazzano, M.; Thiyagarajan, S.; Lotti, N. Poly(butylene
679 2,4-furanoate), an Added Member to the Class of Smart Furan-Based Polyesters for
680 Sustainable Packaging: Structural Isomerism as a Key to Tune the Final Properties. *ACS*
681 *Sustainable Chem. Eng*. **2021**, *9*, 11937–11949.
682 48. Thiyagarajan, S.; Meijlink, M. A.; Bourdet, A.; Vogelzang, W.; Knoop, R. J. I.; Esposito, A.;
683 Dargent, E.; van Es, D. S.; van Haveren, J. Synthesis and Thermal Properties of Bio-Based
684 Copolyesters from the Mixtures of 2,5- and 2,4-Furandicarboxylic Acid with Different Diols.
685 *ACS Sustainable Chem. Eng*. **2019**, *7*, 18505–18516.

686 49. Nolasco, M. M.; Araujo, C. F.; Thiyagarajan, S.; Rudić, S.; Vaz, P. D.; Silvestre, A. J. D.;
687 Ribeiro-Claro, P. J. A.; Sousa, A. F. Asymmetric Monomer, Amorphous Polymer? Structure–
688 Property Relationships in 2,4-FDCA and 2,4-PEF. *Macromolecules* **2020**, *53*, 1380–1387.
689 50. Robertson, G. L. *Food Packaging Principles and Practice*, 3rd Edition, CRC Press, **2013**,
690 Chapter 2-4.
691 51. Davidson, M. G.; Elgie, S.; Parsons, S.; Young, T. J. Production of HMF, FDCA and their
692 derived products: a review of life cycle assessment (LCA) and techno-economic analysis
693 (TEA) studies. *Green Chem*. **2021**, *23*, 3154-3171.
694 52. Bozell, J. J.; Petersen, G. R. Technology development for the production of biobased products
695 from biorefinery carbohydrates—the US Department of Energy's "Top 10" revisited. *Green*
696 *Chem*. **2010**, *12*, 539-554.
697 53. Bio-Based Chemicals A 2020 Update, IEA Bioenergy, available online:
698 https://www.ieabioenergy.com/wp-content/uploads/2020/02/Bio-based-chemicals-a-2020-
699 update-final-200213.pdf (accessed September 2021).
700 54. Zheng, M.; Li, X. Y.; Guan, R. Q.; Liu, Y. M.; Zhao, Y. J.; Tai, Y. L. Ionic Liquid-Catalyzed
701 Synthesis of Diethylene Glycol. *Adv. Mat. Res*. **2012**, *549*, 287-291.
702 55. Bioplastics market data, European-bioplastics.org (accessed September 2021).
703 56. Soccio, M.; Lotti, N.; Finelli, L.; Gazzano, M.; Munari, A. Influence of transesterification
704 reactions on the miscibility and thermal properties of poly(butylene/diethylene succinate)
705 copolymers. *Eur. Polym. J*. **2008**, *44*, 1722-1732.
706 57. Soccio, M.; Lotti, N.; Gigli, M.; Finelli, L.; Gazzano, M.; Munari, A. Reactive blending of
707 poly(butylene succinate) and poly(triethylene succinate): characterization of the copolymers
708 obtained. *Polym. Int*. **2012**, *61*, 1163-1169.
709 58. Fabbri, M.; Gigli, M.; Gamberini, R.; Lotti, N.; Gazzano, M.; Rimini, B.; Munari, A.
710 Hydrolysable PBS-based poly(ester urethane)s thermoplastic elastomers. *Polym. Degrad.*
711 *Stab*. **2014**, *108*, 223-231.

59. Lotti, N.; Finelli, L.; Fiorini, M.; Righetti, M. C.; Munari, A. Synthesis and characterization of poly(butylene terephthalate-co-diethylene terephthalate) copolyesters. *Polymer* **2000**, 41, 5297-5304.

60. Lotti, N.; Finelli, L.; Fiorini, M.; Righetti, M. C.; Munari, A. Synthesis and characterization of poly(butylene terephthalate-co-triethylene terephthalate) copolyesters. *J. Appl. Polym. Sci.* **2001**, *81*, 981-990.

61. Gigli, M.; Lotti, N.; Gazzano, M.; Finelli, L.; Munari, A. Novel eco-friendly random copolyesters of poly(butylene succinate) containing ether-linkages. *React. Funct. Polym*. **2012**, *72*, 303-310.

62. Gigli, M.; Lotti, N.; Gazzano, M.; Siracusa, V.; Finelli, L.; Munari, A.; Dalla Rosa, M. Fully aliphatic copolyesters based on poly(butylene 1,4-cyclohexanedicarboxylate) with promising mechanical and barrier properties for food packaging applications. *Ind. Eng. Chem. Res*. **2013**, *52*, 12876−12886.

63. Gigli, M.; Lotti, N.; Gazzano, M.; Siracusa, V.; Finelli, L.; Munari, A.; Dalla Rosa, M. Biodegradable aliphatic copolyesters containing PEG-like sequences for sustainable food packaging applications. *Polym. Degrad. Stab*. **2014**, *105*, 96-106.

64. Kainulainen, T. P.; Hukka, T. I.; Ozeren, H. D.; Sirvio, J. A.; Hedenqvist, M. S.; Heiskanen, J. P. Utilizing Furfural-Based Bifuran Diester as Monomer and Comonomer for High-Performance Bioplastics: Properties of Poly(butylene furanoate), Poly(butylene bifuranoate), and Their Copolyesters. *Biomacromolecules* **2020**, *21*, 743−752.

65. Jiang, Y.; Woortman, A. J. J.; Alberda van Ekensteina, G. O. R.; Loos, K. A biocatalytic approach towards sustainable furanic–aliphatic polyesters. *Polym. Chem*. **2015**, *6*, 5198-5211.

66. Haernvall, K.; Zitzenbacher, S.; Amer, H.; Zumstein, M. T.; Sander, M.; McNeill, K.; Yamamoto, M.; Schick, M. B.; Ribitsch, D.; Guebitz, G. M. Polyol Structure Influences Enzymatic Hydrolysis of Bio-Based 2,5-Furandicarboxylic Acid (FDCA) Polyesters. *Biotechnol. J*. **2017**, *12*, 1600741.

738 67. Papageorgiou, G. Z.; Papageorgiou, D. G.; Terzopoulou, Z.; Bikiaris, D. N. Production of bio-
739 based 2,5-furan dicarboxylate polyesters: Recent progress and critical aspects in their
740 synthesis and thermal properties. *Eur. Polym. J.* **2016**, *83*, 202-229.
741 68. Tsanaktsis, V.; Terzopoulou, Z.; Nerantzaki, M.; Papageorgiou, G. Z.; Bikiaris, D. N. New
742 poly(pentylene furanoate) and poly(heptylene furanoate) sustainable polyesters from diols
743 with odd methylene groups. *Mater. Lett.* **2016**, *178*, 64-67.
744 69. Diao, L.; Su, K.; Li, Z.; Ding, C. Furan-based co-polyesters with enhanced thermal properties:
745 poly(1,4-butylene-co-1,4-cyclohexanedimethylene-2,5-furandicarboxylic acid) *RSC Adv.*
746 **2016**, *6*, 27632-27639.
747 70. Cottrell, T. L. *The Strengths of Chemical Bonds*, Butterworths, 2nd ed., London, 1958.
748 71. Martinez-Tong, D. E.; Soccio, M.; Robles-Hernández, B.; Guidotti, G.; Gazzano, M.; Lotti,
749 N.; Alegria, A. Evidence of Nanostructure Development from the Molecular Dynamics of
750 Poly(pentamethylene 2,5-furanoate). *Macromolecules* **2020**, *53*, 10526-10537.
751 72. Araujo, C. F.; Nolasco, M. M.; Ribeiro-Claro, P. J. A.; Rudic, S.; Silvestre, A. J. D.; Vaz, P.
752 D.; Sousa, A. F. Inside PEF: chain conformation and dynamics in crystalline and amorphous
753 domains. *Macromolecules* **2018**, *51*, 3515–3526.
754 73. Patkar, M.; Jabarin, S. A. Effect of diethylene glycol (DEG) on the crystallization behavior
755 of poly(ethylene terephthalate) (PET). *J. Appl. Polym. Sci*. **1993**, *47*, 1749-1763.
756 74. Soccio, M.; Lotti, N.; Finelli, L.; Gazzano, M.; Munari, A. Aliphatic poly(propylene
757 dicarboxylate)s: Effect of chain length on thermal properties and crystallization kinetics.
758 *Polymer* **2007**, *48*, 3125-3136.
759 75. Liang, H.; Hao, Y.; Liu, S.; Zhang, H.; Li, Y.; Dong, L.; Zhang, H. Thermal, rheological, and
760 mechanical properties of polylactide/poly(diethylene glycol adipate). *Polym. Bull*. **2013**, *70*,
761 3487–3500.
762 76. Cao, A.; Okamura, T.; Nakayama, K.; Inoue, Y.; Masuda, T. Studies on syntheses and
763 physical properties of biodegradable aliphatic poly(butylene succinate-co-ethylene

764 succinate)s and poly(butylene succinate-co-diethylene glycol succinate)s. *Polym. Degrad.*
765 *Stab*. **2002**, *78*, 107-117.
766 77. Zeng, J. B.; Huang, C. L.; Jiao, L.; Lu, X.; Wang, Y. Z.; Wang, X. L. Synthesis and Properties
767 of Biodegradable Poly(butylene succinate-co-diethylene glycol succinate) Copolymers. *Ind.*
768 *Eng. Chem. Res*. **2012**, *51*, 12258–12265.
769 78. Rudyak, V. Y.; Gavrilov, A. A.; Guseva, D. V.; Tung, S. H.; Komarov, P. V. Accounting for
770 π–π stacking interactions in the mesoscopic models of conjugated polymers. *Mol. Syst. Des.*
771 *Eng.* **2020**, *5*, 1137.
772 79. Sago, T.; Itagaki, H.; Asano, T. Onset of Forming Ordering in Uniaxially Stretched
773 Poly(ethylene terephthalate) Films Due to π−π Interaction Clarified by the Fluorescence.
774 *Macromolecules* **2014**, *47*, 217−226.
775 80. Shanavas, A.; Sathiyaraj, S.; Chandramohan, A.; Narasimhaswamy, T.; Sultan Nasar, A.
776 Isophthalic acid based mesogenic dimers: Synthesis and structural effects on mesophase
777 properties. *J. Mol. Struct*. **2013**, *1038*, 126-133.
778 81. Mahendrasingam, A.; Blundell, D. J.; Martin, C.; Urban, V.; Narayanan, T.; Fuller, W. Time
779 resolved WAXS study of the role of mesophase in oriented crystallisation of poly(ethylene
780 terephthalate-co-isophthalate) copolymers. *Polymer* **2005**, *46*, 6044-6049.
781 82. Nolasco, M. M.; Araujo, C. F.; Thiyagarajan, S.; Rudić, S.; Vaz, P. D.; Silvestre, A. J. D.;
782 Ribeiro-Claro, P. J. A.; Sousa, A. F. Asymmetric Monomer, Amorphous Polymer? Structure–
783 Property Relationships in 2,4-FDCA and 2,4-PEF. *Macromolecules* **2020**, *53*, 1380−1387.
784 83. (Burgess, S. K.; Leisen J. E.; Kraftschik, B. E.; Mubarak, C. R., Kriegel, R. M.; Koros, W. J.
785 Chain Mobility, Thermal, and Mechanical Properties of Poly(ethylene furanoate) Compared
786 to Poly(ethylene terephthalate). *Macromolecules* **2014**, *47*, 1383−1391.
787 84. Bourdet, A.; Esposito, A.; Thiyagarajan, S.; Delbreilh, L.; Affouard, F.; Knoop, R. J. I.;
788 Dargent, E. Molecular Mobility in Amorphous Biobased Poly(ethylene 2,5-

furandicarboxylate) and Poly(ethylene 2,4-furandicarboxylate). *Macromolecules* **2018**, *51*, 1937−1945.

85. Hedenqvist, M. S. Barrier Packaging Materials, in: Kutz, M. (Ed.), *Handbook of Environmental Degradation of Materials*, Elsevier Inc., 2nd ed., **2012**, pp. 833–860.
86. Burgess, S. K.; Kriegel, R. M.; Koros, W. J. Carbon dioxide sorption and transport in amorphous poly (ethylene furanoate). *Macromolecules* **2015**, *48*, 2184–2193.
87. Guidotti, G.; Genovese, L.; Soccio, M.; Gigli, M.; Munari, A.; Siracusa, V.; Lotti, N. Block Copolyesters Containing 2,5-Furan and trans-1,4-Cyclohexane Subunits with Outstanding Gas Barrier Properties. *Int. J. Mol. Sci.* **2019**, *20*, 1–15.
88. Guidotti, G.; Soccio, M.; Lotti, N.; Gazzano, M.; Siracusa, V.; Munari, A. Poly (propylene 2, 5-thiophenedicarboxylate) vs. Poly (propylene 2, 5-furandicarboxylate): Two examples of high gas barrier bio-based polyesters. *Polymers* **2018**, *10*, 785.
89. Guidotti, G.; Gigli, M.; Soccio, M.; Lotti, N.; Gazzano, M.; Siracusa, V.; Munari, A. Ordered structures of poly (butylene 2, 5-thiophenedicarboxylate) and their impact on material functional properties. *Eur. Polym. J.* **2018**, *106*, 284–290.